LA-UR-98-3527

Los Alamos National Laboratory is operated by the University of California for the US Department of Energy under contract W-7405-ENG-36.

TITLE: GASFLOW SIMULATIONS OF FLOW IN BUILDINGS

AUTHOR(S): CATHRIN MÜLLER, DENNIS R. LILES, JAY W. SPORE, AND GEORGE F. NIEDERAUER

SUBMITTED TO: 2ND AMS CONF. ON THE URBAN ENVIRONMENT ALBUQUERQUE, N.M., NOV. 1998

Los Alamos National Laboratory
Los Alamos, New Mexico
87545

1.1 GASFLOW SIMULATIONS OF FLOW IN BUILDINGS

Cathrin Müller,* Dennis R. Liles, Jay W. Spore, and George F. Niederauer
Los Alamos National Laboratory

1. INTRODUCTION

The goal of these simulation studies was to demonstrate the capability of the GASFLOW computer code to predict detailed concentration distributions of toxic gases released in a subway station and in an airplane hangar, which represents an open building like a gymnasium. The predicted time behavior of gas release and distribution can be used for determining sensor locations, developing emergency response plans, and training first responders.

GASFLOW, Travis (1994), is a finite-volume computer code for solving transient, three-dimensional, compressible, Navier-Stokes equations for multiple gas species. It calculates the transport, mixing, and combustion of flammable gases and aerosols in geometrically complex domains. GASFLOW has been used for many years to perform best-estimate safety analyses by the Nuclear Regulatory Commission, the Department of Energy, and international agencies.

2. SUBWAY SIMULATION

The subway station is ~18 m wide, 184 m long, and 9 m high (60 ft wide, 600 ft long, and 30 ft high). There are two tracks: inbound and outbound. A full-length train is assumed to be in the station on the inbound track. Another train is upstream away from the station on the outbound track. For ~30 m past each end of the station, the tracks in the tunnel are separated only by a series of support columns so that incoming and outgoing flow interact in the tunnel to a certain extent in the tunnel near the station. After ~30 m, the tunnels for the inbound and outbound tracks are enclosed separately. Thus, in the model a tunnel of 30 m was added to each end so that separate boundary conditions could be supplied for each of the four tunnels.

Within the station, eight platform escalators take passengers between the platform and mezzanine. At each end of the station, a set of street escalators carry passengers to and from the surface level. The street escalator shafts are ~24 m x 7 m x 9 m (80 ft x 23 ft x 30 ft).

The station was modeled in Cartesian coordinates with 35,976 cells, as shown in Fig. 1. Internal structures (columns, mezzanines, and platform escalators) and a train in the station were described by obstacles. (An obstacle is a solid cell that has no flow through it.) A nonuniform grid was used to capture internal structures. Grid sizes range from 70 cm to 4.2 m (2.3 ft to 13.8 ft). Parapets and platform extensions over supporting structures were modeled as solid surfaces, which allowed no flow between cells.

* Corresponding author address: Cathin Müller, Los Alamos National Laboratory, TSA-10, MS K575, Los Alamos, NM 87545; email: cmuller@lanl.gov.

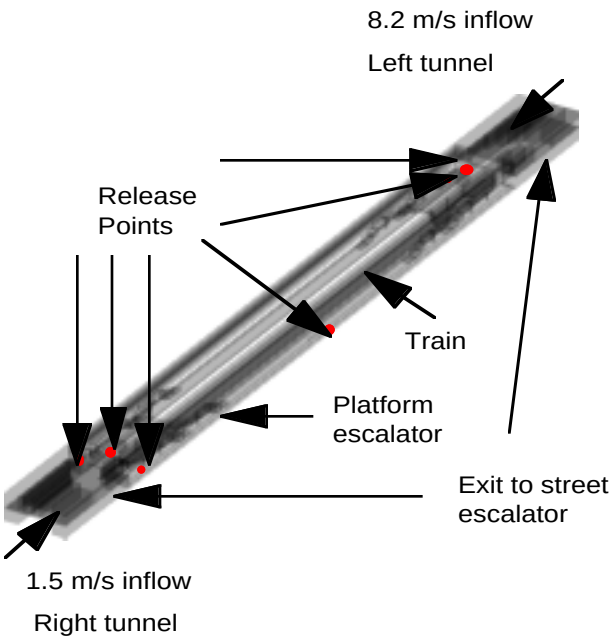

Fig. 1. GASFLOW model of subway station.

Initial conditions for the air in the station and escalator shafts were set to a temperature of 300 K and a pressure of 0.1 MPa. Atmospheric pressure boundary conditions were applied where the escalator shafts reach the street level. An algebraic turbulence model was used in all calculations. Heat transfer to the walls or from the train was ignored.

Scenarios

Two main situations were considered, each with multiple cases. The first one was a bounding situation, where maximum and minimum inflow velocities were used as time-independent boundary conditions. In the second situation, the velocity boundary conditions were time-dependent and describe a more realistic sequence during rush hour. The inflow velocities used for boundary conditions are based on results from an SES code simulation carried out at Argonne National Laboratory.

To form a common initial condition for all cases, a steady-state calculation was performed to establish a developed flow field before any agents were released. It took ~400 s real time to reach steady state. We observe a very complex flow field with a strong flow down the platform on the outbound track and up to the mezzanine. Because of many internal structures, the

flow is highly turbulent, and recirculation areas and reverse flow can be seen. For each case, 100 g of the agent (gas) was released over a period of 10 s, i.e., from 400 to 410 s. The simulations were run for 200 s after initiating the releases.

a) Bounding situation

The boundary conditions in this situation are a low inflow velocity of ~1.5 m/s (5 ft/s) at the tunnel entrance to the inbound track with a train at the station, and a high inflow velocity of ~8.2 m/s (27 ft/s) at the tunnel entrance to the outbound track with no train at the station. Zero-gradient boundary conditions were imposed to model continuous flow at the corresponding opposite tunnels of the station.

A neutral agent was released after reaching steady state. For the first case, the source was placed on the platform near the platform escalator closest to the entrance tunnel of the outbound track. This was an area of high inflow velocity. The calculation was run for 200 s. The agent is convected both up to the mezzanine and down the empty platform in ~20 to 30 s. The other platform is effectively shielded by the train. The gas reaches the street escalators after 60 to 80 s. Then the gas agent exits through the escalators on both ends to the surface. Most of the gas has left the station ~2 min after the release.

Several other cases were run to examine the effect of different source locations, different weight gas agents, and multiple releases. Agent sources were placed at six different locations: near the platform escalators at the beginning and the end of the platform of the outbound track, near the beginning of the inbound platform (where the train sits and the inflow velocity is low), near the kiosks on the mezzanine at both ends of the station, and in the center of the inbound platform. In some cases the location was the same; however, the neutral gas was substituted with a heavier gas, which had a molecular weight representing propylene. It could be seen that the heavier gas took slightly longer to reach the exits and would remain at the platform level longer. However, the main difference was determined by the source location. When the gas was released at the low-velocity end of the outbound platform, it took only 20 s to reach the nearest exit. It would then slowly travel down both platforms and not even reach the exit passageway at the other end within 200 s. When the source was located in the center of the inbound platform (the side with the train), it took 2 min for the gas to reach the mezzanine level.

b) Time-dependent velocities situation

Two sets of cases were run in which the velocity boundary conditions imposed at the tunnel were time dependent. In one set of cases, a time-dependent inflow velocity boundary condition was applied; in the other set of cases a time-dependent outflow condition was imposed. Each set contained four cases: a neutral gas released at the high-velocity entrance, at the low-velocity entrance (train), at the kiosk at the low- velocity end of station, and a heavy gas released at the kiosk at the high-velocity end of the station. The velocity curves describe arriving and departing trains during rush hour; maxima and minima are 90 s apart.

Recirculation areas develop around the street escalators. In the street escalator shafts, some reverse flow from the outside develops, but it occurs only for a very short time so no significant amount of fresh air is brought into the station.

The gas remains in the station longer than in the bounding situation and in some cases does not reach either exit within the simulation time of 200 s. Also, the distribution is more even around the source area because the flow speeds up and slows down periodically. See Table 1 for a comparison of some cases with the bounding situation. The “a” stands for the bounding situation; “b” stands for the one with time-dependent velocity boundary conditions. The third and fourth columns describe how many seconds it took the maximum amount of the gas to reach certain locations in the station after the release starts at 400 s.

Because an agent distributes quickly, the most important conclusions are that sensors need to be placed advantageously for fast detection, and emergency actions need to be taken quickly, in a range from ~20 s to a few minutes.

3. HANGAR SIMULATION

The hangar is ~39 m (128 ft) wide, 49 m (160 ft) long, and 10 m (33 ft) high. The 10 sliding hangar doors on the north side, measuring 7 m (23 ft) high and 33 m (108 ft) wide, form the main leakage path, with

TABLE 1. Time to reach maximum concentration at certain locations after agent release.

Case	Release Location	time (s) to reach Mezzanine East / West	time (s) to reach Exits East / West
a.1	East Kiosk (high v)	25 / > 200	60 / >200
a.2	end outbound platform (no train, low v)	>200 / 20	>200 / 50
a.3	beginning outbound platform (no train, high v)	20 / 70	60 / 80
b.1	East Kiosk (high v)	45 / 200	135 / >200
b.2	beginning inbound platform (train, low v)	200 / 200	>200 / >200
b.3	beginning outbound platform (no train, high v)	70 / >200	200 / > 200

especially large gaps on the left side and bottom of the fifth door just east of the center. On the south side of the hangar is a hallway with a door to the exterior. The ventilation system inside the hangar has an outside air inlet, a return duct, and three supply ducts. A curtain that can separate the north and south sides of the building was fully open to ~24 m (79 ft) wide and 4 m (13 ft) high. Two sensors are located at a height of 2 m (6.5 ft) on the north side of the building, asymmetrically on the east and west sides of the north duct leg.

The GASFLOW model (see Fig. 2) used 12,096 cells for the hangar interior and 2016 cells added in front of the doors to capture the flow characteristics from the wind. Cell sizes range from 0.6 to 2 m (2 to 6.5 ft). The wind was measured at 10 m (33 ft) above ground. Velocity profiles were computed and used as the north boundary conditions using a power law and a boundary layer that are characteristic for urban environments. The released aerosol was modeled as a heavy gas. Several sensitivity cases were run to compare individual effects with the base, which used the conditions for the June 1997 test at Dugway and included variable winds.

Scenarios

Eight different cases were considered:

1. Base Case—The actual conditions for the June 1997 test (i.e., time-dependent wind data) were used.
2. Case 1—The wind condition is dead calm.
3. Case 2—Stiff, constant wind at 5 m/s (16.4 ft), in a single head-on direction toward the hangar door.
4. Case 3—HVAC flow rate +20% over base case.
5. Case 4—HVAC flow rate -50% of base case.
6. Case 5—Leakage +20% of base case.
7. Case 6—Leakage -20% of base case.
8. Case 7—Leakage reversed for hangar doors and outside air vent.

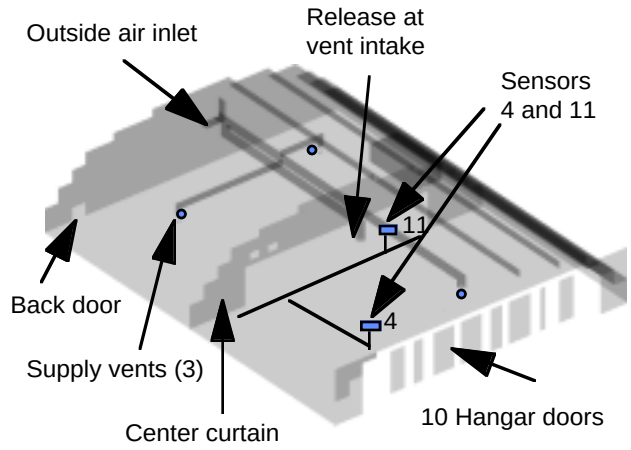

Fig. 2. Perspective view of hangar model. (Openings for back door, hangar doors, and curtain are larger than actual size. A fractional area model was used to model actual flow area. A typical fraction for leakage is ~2%. The block behind the curtain is a closed-off work room, modeled as a set of obstacles.)

A steady-state calculation was performed to establish a developed flow field before any agent was released. This was done for all of the different cases. This was more important for the changing flow rates in the HVAC system that influence the flow field in the hangar than for the changing outside wind conditions.

We observed velocities of ~5 cm/s (2 in./s) in the vicinity of the sensors. The main flow field showed downward flow away from the vents and several recirculation areas. The flow of air leaking to the outside through the hangar doors was enhanced by upward flow outside the hangar. Upward flow occurred when the wind curved up just in front of the building.

After reaching steady state, a gas representing 98 g of aerosol was released in the return duct. Ninety percent of the agent was released in the first 30 s and the remaining ten percent in the next 30 s. The calculations were run out to 10 min in real time because this is the period for which computational fluid dynamics (CFD) codes are most useful.

GASFLOW calculated the first and highest concentration peaks for sensor 11 at 213 s, and at sensor 4 at 230 s in the base case (see Fig. 3). Around 400 s for sensor 11 and 500s for sensor 4, secondary lower and wider peaks occurred, after which the concentration decreased.

In the case where there was no wind, the results are very similar to the base case. The first peak was wider, and the secondary peak was much less pronounced.

In the case with a constant wind of 5 m/s blowing towards the hangar, the much stronger and constant wind in front of the hangar has a big influence on the results. At sensor 4, no outstanding peak was reached at all, and the peak at location 11 was much lower.

In the case where the HVAC flow rate was increased by 20%, the peak at sensor 11 occurred ~100 s earlier—the earliest for all cases—because of increased flow. However, the maximum value was only

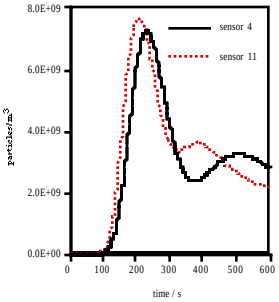

Fig. 3. Total particles vs time. Base case.

~60% of the base value. The peak at sensor 4 was 30 s earlier and 26% higher.

In case 4 where the HVAC flow rate was decreased by 50% (see Fig. 4), the peak at sensor 4 was the highest for all cases, and for once occurred before the

peak at sensor 11. The peak was 37% higher than in the base case.

In the cases where the hangar leakage was increased or decreased by 20%, the behavior was almost identical to the base case.

For a reversed leakage, the maximum values are reached earlier at both locations. The maximum at sensor 4 was 15% higher than in the base case. At location 11, the maximum value was 35% lower than in the base case.

The sensor locations were not symmetric in relation to the ducts, so different peak times for the sensors were seen. We observed a downward flow at the duct exits; the agent spread across the floor first and then moved upward based on the created turbulence. This turbulence was dependent on the flow field, which in turn strongly depended on the flow rate in the HVAC system. The biggest difference in the results compared with the base case was observed for cases 3 and 4 where the flow in the HVAC system was changed. In case of a lower flow rate in the HVAC, there were earlier and higher peaks, which was caused by less turbulence and a longer time for particle buildup. Also, for a high wind of 5 m/s (case 2, as opposed to ~0.5 m/s in the base case) outside the hangar and a change in leakage of about one order of magnitude (case 7, reversed leakage), we can see significant changes caused by a changed flow pattern inside the hangar.

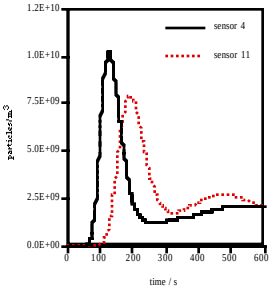

Fig. 4. Total particles vs time. HVAC flow rate was decreased by 50%.

4. CONCLUSIONS

GASFLOW is a valuable tool for simulating and visualizing the release and distribution of agents in buildings, especially in situations where one needs to characterize local phenomena within a flow field. The results show complex flow and concentration fields caused by internal structures, boundary conditions, and active systems, such as subway trains and HVAC systems. Because a gas distributes quickly, the most important conclusions are that sensors need to be placed advantageously for fast detection, and emergency actions need to be taken quickly, in a range from some 20 s to a few minutes. Insights gained from three-dimensional visualization of scenes of invisible gases or opaque clouds would be invaluable for determining sensor locations, developing emergency response plans, and training first responders.

5. REFERENCES

Travis, J. R., Lam, K. L., and Wilson, T. L., 1994: GASFLOW: A Three-Dimensional Finite-Volume Fluid-Dynamics Code for Calculating the Transport, Mixing, and Combustion of Flammable Gases in Geometrically Complex Domains, LA-UR-94-2270.